(12) INTERNATIONAL APPLICATION PUBLISHED UNDER THE PATENT COOPERATION TREATY (PCT)

(19) World Intellectual Property Organization
International Bureau

(43) International Publication Date
18 May 2007 (18.05.2007)

PCT

(10) International Publication Number
WO 2007/056427 A2

(51) International Patent Classification:
G11B 5/64 (2006.01)

(21) International Application Number:
PCT/US2006/043435

(22) International Filing Date:
7 November 2006 (07.11.2006)

(25) Filing Language: English

(26) Publication Language: English

(30) Priority Data:
11/268,547 8 November 2005 (08.11.2005) US

(71) Applicant *(for all designated States except US)*: **MASSACHUSETTS INSTITUTE OF TECHNOLOGY** [US/US]; 77 Massachusetts Avenue, Cambridge, MA 02142-1324 (US).

(72) Inventors; and
(75) Inventors/Applicants *(for US only)*: **ZHAI, Lei** [CN/US]; 12424 Research Parkway, Suite 400, Orlando, FL 328826 (US). **COHEN, Robert, E.** [US/US]; 73 Pershing Road, Jamaica Plain, MA 02130-2015 (US). **RUBNER, Michael, F.** [US/US]; 12 Lynwood Lane, Westford, MA 01886 (US). **CEBECI, Fevzi, C.** [TR/US]; Istanbul Teknik Universitesi Fen, Edebiyat Fakultesi, Kimya Bolumu, 34469 Maslak, Istanbul xx (TR).

(74) Agents: **FOX, Harold, H.** et al.; STEPTOE & JOHNSON LLP, 1330 Connecticut Avenue, NW, Washington, DC 20036 (US).

(81) Designated States *(unless otherwise indicated, for every kind of national protection available)*: AE, AG, AL, AM, AT, AU, AZ, BA, BB, BG, BR, BW, BY, BZ, CA, CH, CN, CO, CR, CU, CZ, DE, DK, DM, DZ, EC, EE, EG, ES, FI, GB, GD, GE, GH, GM, GT, HN, HR, HU, ID, IL, IN, IS, JP, KE, KG, KM, KN, KP, KR, KZ, LA, LC, LK, LR, LS, LT, LU, LV, LY, MA, MD, MG, MK, MN, MW, MX, MY, MZ, NA, NG, NI, NO, NZ, OM, PG, PH, PL, PT, RO, RS, RU, SC, SD, SE, SG, SK, SL, SM, SV, SY, TJ, TM, TN, TR, TT, TZ, UA, UG, US, UZ, VC, VN, ZA, ZM, ZW.

(84) Designated States *(unless otherwise indicated, for every kind of regional protection available)*: ARIPO (BW, GH, GM, KE, LS, MW, MZ, NA, SD, SL, SZ, TZ, UG, ZM, ZW), Eurasian (AM, AZ, BY, KG, KZ, MD, RU, TJ, TM), European (AT, BE, BG, CH, CY, CZ, DE, DK, EE, ES, FI, FR, GB, GR, HU, IE, IS, IT, LT, LU, LV, MC, NL, PL, PT, RO, SE, SI, SK, TR), OAPI (BF, BJ, CF, CG, CI, CM, GA, GN, GQ, GW, ML, MR, NE, SN, TD, TG).

Published:
— *without international search report and to be republished upon receipt of that report*

For two-letter codes and other abbreviations, refer to the "Guidance Notes on Codes and Abbreviations" appearing at the beginning of each regular issue of the PCT Gazette.

WO 2007/056427 A2

(54) Title: SUPERHYDROPHILIC COATINGS

(57) Abstract: A superhydrophilic coating can be antireflective and antifogging. The coating can remain antireflective and antifogging for extended periods.

SUPERHYDROPHILIC COATINGS

FEDERALLY SPONSORED RESEARCH OR DEVELOPMENT

The U.S. Government may have certain rights in this invention pursuant to Grant Nos. CTS-9729569 and DMR-9808941 awarded by the National Science Foundation.

TECHNICAL FIELD

This invention relates to superhydrophilic coatings.

BACKGROUND

Polyelectrolyte multilayers can be easily assembled on a variety of surfaces. Selection of the materials, assembly conditions, and post-processing conditions can be used to control the chemical, structural and optical properties of the final product.

SUMMARY

Stable superhydrophilic coatings can be formed from layer-by-layer assembled films including nanoparticles and polyelectrolytes. The superhydrophilic coatings can be antifogging, antireflective, or both anti-fogging and anti-reflective.

In one aspect, a superhydrophilic surface includes a nanotextured coating including a hydrophilic material arranged on a substrate. The coating can be a partial coating, i.e., a coating that coats a portion of the substrate. The substrate can be substantially transparent, and the surface can be substantially transparent. The surface can have a refractive index of less than 1.4, or of less than 1.3. The coating can have a thickness of less than 500 nm, or of less than 300 nm. The surface can have an rms roughness in the range of 10-20 nm, or in the range of 12-16 nm.

The coating can include a plurality of nanoparticles. The plurality of nanoparticles can include a silica nanoparticle. The plurality of nanoparticles can include a nanoparticle having a diameter in the range of 5 nm to 100 nm, or in the range of 5 nm to 25 nm.

The coating can be substantially free of organic polymer. The coating can includes a polyelectrolyte. The polyelectrolyte can include a polycation. The polyelectrolyte can include poly(allylamine hydrochloride).

The coating can further include a bilayer, the bilayer including a polyelectrolyte having a charge and a material having an opposite charge. The material having the opposite charge can be a polyelectrolyte. The material having the opposite charge can be a plurality of nanoparticles.

In another aspect, a method of treating a surface includes forming a coating on a surface of a substrate, wherein the coating includes a bilayer including a polyelectrolyte having a charge and a second material having an opposite charge. The second material can be hydrophilic. The second material can include a polyelectrolyte. The second material can include a nonpolymeric material. The second material can include a plurality of nanoparticles.

The method can include sequentially forming a plurality of bilayers, wherein each bilayer includes a polyelectrolyte having a charge and a second material having an opposite charge.

At least one bilayer can include a polyelectrolyte. At least one bilayer can include a nonpolymeric material. At least one bilayer can include a plurality of nanoparticles.

Forming the bilayer can include contacting the surface of the substrate with an aqueous solution of the polyelectrolyte. Forming the bilayer can include contacting the surface of the substrate with an aqueous solution of the second material. The method can include heating the coating. The method can include contacting the coating with a plasma.

In another aspect, a method of manufacturing an antifogging surface includes forming a nanotextured coating including a hydrophilic material arranged on a surface of a substrate.

In another aspect, an article includes a surface having an antireflective coating including a nanotextured hydrophilic material.

In another aspect, an article includes a surface having an antifogging coating including a nanotextured hydrophilic material.

The details of one or more embodiments are set forth in the accompanying drawings and the description below. Other features, objects, and advantages will be apparent from the description and drawings, and from the claims.

BRIEF DESCRIPTION OF THE DRAWINGS

FIGS. 1A and 1B are scanning electron microscope images of porous polyelectrolyte multilayers.

FIG. 2 is a graph depicting water contact angles for different surfaces.

FIG. 3A is a scanning electron microscope image of a superhydrophobic surface. FIG. 3B is a photograph of a water droplet on the superhydrophobic surface.

FIGS. 4A and 4B are graphs depicting X-ray photoelectron spectroscopy measurements of surfaces.

FIG. 5A is a graph depicting film thickness measurements as a function of number of bilayers. FIG. 5B is a graph depicting refractive index measurements as a function of number of bilayers. FIG. 5C is a graph depicting film thickness and refractive index measurements as a function of number of bilayers.

FIG. 6 is an AFM image of a superhydrophilic surface.

FIG. 7 is a graph depicting transmittance and thickness measurements for films having different numbers of bilayers.

FIGS. 8A and 8B are graphs depicting transmittance and reflectance spectra for glass slides coated with polyelectrolyte multilayers.

FIG. 9A is a series of video images of water drops falling on a superhydrophilic surface. FIGS. 9B and 9C are graphs depicting contact angle measurements as a function of time for different surfaces.

FIG. 10 is a graph depicting contact angle measurements for surfaces under different conditions.

FIG. 11A is a photograph comparing fogging behavior of glass slides with different surfaces. FIG. 11B is a photograph illustrating dewetting behavior of a partially coated glass slide.

DETAILED DESCRIPTION

Surfaces having a nanotexture can exhibit extreme wetting properties. A nanotexture refers to surface features, such as ridges, valleys, or pores, having nanometer (i.e., typically less than 1 micrometer) dimensions. In some cases, the features will have an average or rms dimension on the nanometer scale, even though some individual features may exceed 1 micrometer in size. The nanotexture can be a 3D network of

interconnected pores. Depending on the structure and chemical composition of a surface, the surface can be hydrophilic, hydrophobic, or at the extremes, superhydrophilic or superhydrophobic. One method to create the desired texture is with a polyelectrolyte multilayer. Polyelectrolyte multilayers can also confer desirable optical properties to surfaces, such as anti-reflectivity, or reflectivity in a desired range of wavelengths. See, for example, U.S. Patent Application Publication No. 2003/0215626, and U.S. Patent Application No. 10/912,540, each of which is incorporated by reference in its entirety.

Hydrophilic surfaces attract water; hydrophobic surfaces repel water. In general, a non-hydrophobic surface can be made hydrophobic by coating the surface with a hydrophobic material. The hydrophobicity of a surface can be measured, for example, by determining the contact angle of a drop of water on the surface. The contact angle can be a static contact angle or dynamic contact angle. A dynamic contact angle measurement can include determining an advancing contact angle or a receding contact angle, or both. A hydrophobic surface having a small difference between advancing and receding contact angles (i.e., low contact angle hysteresis) can be desirable. Water droplets travel across a surface having low contact angle hysteresis more readily than across a surface having a high contact angle hysteresis.

A surface can be superhydrophilic. A superhydrophilic surface is completely and instantaneously wet by water, i.e., exhibiting water droplet advancing contact angles of less than 5 degrees within 0.5 seconds or less upon contact with water. See, for example, Bico, J. et al., *Europhys. Lett.* **2001**, *55*, 214-220, which is incorporated by reference in its entirety. At the other extreme, a surface can be superhydrophobic, i.e. exhibiting a water droplet advancing contact angles of 150° or higher. The lotus leaf is an example of a superhydrophobic surface (See Neinhuis, C.; Barthlott, W. *Ann. Bot.* **1997**, *79*, 677; and Barthlott, W.; Neinhuis, C. *Planta* **1997**, *202*, 1, each of which is incorporated by reference in its entirety). The lotus leaf also exhibits very low contact angle hysteresis: the receding contact angle is within 5° of the advancing contact angle (See, for example, Chen, W.; et al. *Langmuir* **1999**, *15*, 3395; and Oner, D.; McCarthy, T. J. *Langmuir* **2000**, *16*, 7777, each of which is incorporated by reference in its entirety).

Photochemically active materials such as TiO_2 can become superhydrophilic after exposure to UV radiation; or, if treated with suitable chemical modifications, visible radiation. Surface coatings based on TiO_2 typically lose their superhydrophilic qualities within minutes to hours when placed in a dark environment, although much progress has

been made towards eliminating this potential limitation. See, for example, Gu, Z. Z.; Fujishima, A.; Sato, O. *Angewandte Chemie-International Edition* 2002, 41, (12), 2068-2070; and Wang, R.; et al., *Nature* 1997, 388, (6641), 431-432; each of which is incorporated by reference in its entirety.

Textured surfaces can promote superhydrophilic behavior. Early theoretical work by Wenzel and Cassie-Baxter and more recent studies by Quéré and coworkers suggest that it is possible to significantly enhance the wetting of a surface with water by introducing roughness at the right length scale. See, for example, Wenzel, R. N. *J. Phys. Colloid Chem.* 1949, 53, 1466; Wenzel, R. N. *Ind. Eng. Chem.* 1936, 28, 988; Cassie, A. B. D.; Baxter, S. *Trans. Faraday Soc.* 1944, 40, 546; Bico, J.; et al., D. *Europhysics Letters* 2001, 55, (2), 214-220; and Bico, J.; et al. *Europhysics Letters* 1999, 47, (6), 743-744, each of which is incorporated by reference in its entirety. Building on this work, it has recently been demonstrated that both lithographically textured surfaces and microporous surfaces can be rendered superhydrophilic. See, e.g., McHale, G.; Shirtcliffe, N. J.; Aqil, S.; Perry, C. C.; Newton, M. I. *Physical Review Letters* 2004, 93, (3), which is incorporated by reference in its entirety. The intriguing possibility of switching between a superhydrophobic and superhydrophilic state has also been demonstrated with some of these surface structures. See, for example, Sun, T. L.; et al. *Angewandte Chemie-International Edition* 2004, 43, (3), 357-360; and Gao, Y. F.; et al. *Langmuir* 2004, 20, (8), 3188-3194, each of which is incorporated by reference in its entirety.

Layer-by-layer processing of polyelectrolyte multilayers can be used to make conformal thin film coatings with molecular level control over film thickness and chemistry. Charged polyelectrolytes can be assembled in a layer-by-layer fashion. In other words, positively- and negatively-charged polyelectrolytes can be alternately deposited on a substrate. One method of depositing the polyelectrolytes is to contact the substrate with an aqueous solution of polyelectrolyte at an appropriate pH. The pH can be chosen such that the polyelectrolyte is partially or weakly charged. The multilayer can be described by the number of bilayers it includes, a bilayer resulting the sequential application of oppositely charged polyelectrolytes. For example, a multilayer having the sequence of layers PAH-PAA-PAH-PAA-PAH-PAA would be said to be made of three bilayers.

These methods can provide a new level of molecular control over the deposition process by simply adjusting the pH of the processing solutions. A nonporous

polyelectrolyte multilayer can form porous thin film structures induced by a simple acidic, aqueous process. Tuning of this pore forming process, for example, by the manipulation of such parameters as salt content (ionic strength), temperature, or surfactant chemistry, can lead to the creation of micropores, nanopores, or a combination thereof. A nanopore has a diameter of less than 150 nm, for example, between 1 and 120 nm or between 10 and 100 nm. A nanopore can have diameter of less than 100 nm. A micropore has a diameter of greater than 150 nm, typically greater than 200 nm. Selection of pore forming conditions can provide control over the porosity of the coating. For example, the coating can be a nanoporous coating, substantially free of micropores. Alternatively, the coating can be a microporous coating having an average pore diameters of greater than 200 nm, such as 250 nm, 500 nm, 1 micron, 2 microns, 5 microns, 10 microns, or larger.

The properties of weakly charged polyelectrolytes can be precisely controlled by changes in pH. See, for example, G. Decher, Science 1997, 277, 1232; Mendelsohn et al., Langmuir 2000, 16, 5017; Fery et al., Langmuir 2001, 17, 3779; Shiratori et al., Macromolecules 2000, 33, 4213; and U.S. Patent Application No. 10/393,360, each of which is incorporated by reference in its entirety. A coating of this type can be applied to any surface amenable to the water based layer-by-layer (LbL) adsorption process used to construct these polyelectrolyte multilayers. Because the water based process can deposit polyelectrolytes wherever the aqueous solution contacts a surface, even the inside surfaces of objects having a complex topology can be coated. In general, a polyelectrolyte can be applied to a surface by any method amenable to applying an aqueous solution to a surface, such as dipping or spraying.

Surfaces with extreme wetting behavior can be fabricated from a polyelectrolyte coating. See, for example, U.S. Patent Application No. 10/912,576, which is incorporated by reference in its entirety. A polyelectrolyte has a backbone with a plurality of charged functional groups attached to the backbone. A polyelectrolyte can be polycationic or polyanionic. A polycation has a backbone with a plurality of positively charged functional groups attached to the backbone, for example poly(allylamine hydrochloride). A polyanion has a backbone with a plurality of negatively charged functional groups attached to the backbone, such as sulfonated polystyrene (SPS) or poly(acrylic acid), or a salt thereof. Some polyelectrolytes can lose their charge (i.e., become electrically neutral)

depending on conditions such as pH. Some polyelectrolytes, such as copolymers, can include both polycationic segments and polyanionic segments.

Superhydrophilic surfaces can be created from multilayer films. Such conformable superhydrophilic surfaces can be used in, for example, antireflective or antifogging applications. Superhydrophobic surfaces can be created from multilayer films. Such conformable superhydrophobic surfaces can have applications as antifouling, self-cleaning and water resistant coatings, as an anti-cell adhesion (e.g., antibacterial) coating, as an electrical or thermal insulating coating, as a flow-increasing coating (e.g., on the interior wall of a pipe) and as coatings for microfluidic channels and biosensors.

Multilayer thin films containing nanoparticles of SiO_2 can be prepared via layer-by-layer assembly (see Lvov, Y.; Ariga, K.; Onda, M.; Ichinose, I.; Kunitake, T. *Langmuir* 1997, 13, (23), 6195-6203, which is incorporated by reference in its entirety). Other studies describe multilayer assembly of TiO_2 nanoparticles, SiO_2 sol particles and single or double layer nanoparticle-based anti-reflection coatings. See, for example, Zhang, X-T.; et al. *Chem. Mater.* **2005**, 17, 696; Rouse, J. H.; Ferguson, G. S. *J. Am. Chem. Soc.* **2003**, *125*, 15529; Sennerfors, T.; et al. *Langmuir* **2002**, *18*, 6410; Bogdanvic, G.; et al. *J. Colloids Interface Science* **2002**, *255*, 44; Hattori, H. *Adv. Mater.* **2001**, *13*, 51; Koo, H. Y.; et al. *Adv. Mater.* **2004**, *16*, 274; and Ahn, J. S.; Hammond, P. T.; Rubner, M. F.; Lee, I. *Colloids and Surfaces A: Physicochem. Eng. Aspects* **2005**, *259*, 45, each of which is incorporated by reference in its entirety. Incorporation of TiO_2 nanoparticles into a multilayer thin film can improve the stability of the superhydrophilic state induced by light activation. See, e.g., Kommireddy, D. S.; et al. *J. Nanosci. Nanotechnol.* **2005**, *5*, 1081, which is incorporated by reference in its entirety.

Broadband antireflectivity can be attained using an inexpensive, simple process employing aqueous solutions of polymers. See, for example, U.S. Patent Application Publication No. 2003/0215626, which is incorporated by reference in its entirety. The process can be used to apply a high-efficiency conformal antireflective coating to virtually any surface of arbitrary shape, size, or material. The process can be used to apply the antireflective coating to more than one surface at a time and can produce coatings that are substantially free of pinholes and defects, which can degrade coating performance. The porous polymeric material can be antireflective. The process can be used to form antireflective and antiglare coatings on polymeric substrates. The simple and highly versatile process can create molecular-level engineered conformal thin films that

function as low-cost, high-performance antireflection and antiglare coatings. The method can uniformly coat both sides of a substrate at once to produce defect and pinhole-free transparent coatings. The process can be used to produce high-performance polymeric optical components, including flat panel displays and solar cells.

Similarly, the polymer coating can be an antifogging coating. The antifogging coating can prevent condensation of light-scattering water droplets on a surface. By preventing the formation of light-scattering water droplets on the surface, the coating can help maintain optical clarity of a transparent surface, e.g., a window or display screen. The coating can be both antireflective and antifogging. A surface of a transparent object having the antifogging coating maintains its transparency to visible light when compared to the same object without the antifogging coating under conditions that cause water condensation on the surface.

A superhydrophilic coating can be made by depositing a polyelectrolyte multilayer film on a substrate and treating the multilayer to induce a porosity transition. The porosity transition can give rise to nanoscale porosity in the multilayer. Nanoparticles can be applied to further augment the texture of the surface. Finally, a hydrophobic material can be applied to render the surface superhydrophobic. Before the hydrophobic material is applied, the surface can be superhydrophilic.

Polyelectrolyte multilayer films have been used as a template to provide the surface roughness of a superhydrophobic surface. A layer-by-layer process was used to assemble a polyelectrolyte multilayer containing SiO_2 nanoparticles. The film was then heated to 650 °C to remove the polyelectrolytes and create the surface texture needed for superhydrophobic behavior (see Soeno, T. et al. *Transactions of the Materials Research Society of Japan* **2003**, *28*, 1207, which is incorporated by reference in its entirety). In another example, dendritic gold clusters were electrochemically deposited onto indium tin oxide (ITO) electrodes covered with a polyelectrolyte multilayer film. After the deposition of a n-dodecanethiol monolayer on the gold clusters, the surface showed superhydrophobic behavior (see Zhang, X. et al. *J. Am. Chem. Soc.* **2004**, *126*, 3064, which is incorporated by reference in its entirety). The electrochemical deposition process used to create these films can limit the types of materials that this method can be used to form a superhydrophobic coating on.

A superhydrophobic surface can include a polyelectrolyte multilayer. A surface can be coated with the multilayer using a layer-by-layer method. Treatment of the

multilayer can induce the formation of roughness in the multilayer. The multilayer can become a high roughness multilayer. High roughness can be micrometer scale roughness. The high roughness surface can have an rms roughness of 100 nm, 150 nm, 200 nm, or greater. Treatments that induce the formation of high roughness can include an acid treatment or a salt treatment (i.e., treatment with an aqueous solution of a salt). Formation of pores in the polyelectrolyte multilayer can lead to the development of high roughness in the multilayer. Appropriate selection of conditions (e.g., pH, temperature, processing time) can promote formation of pores of different sizes. The pores can be micropores (e.g., pores with diameters at the micrometer scale, such as greater than 200 nm, greater than 500 nm, greater than 1 micrometer, or 10 micrometers or later). A microporous polyelectrolyte multilayer can be a high roughness polyelectrolyte multilayer.

A high roughness polyelectrolyte multilayer can be formed by forming the polyelectrolyte multilayer over a high roughness surface. When the polyelectrolyte multilayer is formed over a high roughness surface, a treatment to increase the polyelectrolyte multilayer of the polyelectrolyte multilayer can be optional. The high roughness surface can include, for example: particles, such as microparticles or microspheres; nanoparticles or nanospheres; or an area of elevations, ridges or depressions. The micrometer scale particles can be, for example, particles of a clay or other particulate material. Elevations, ridges or depressions can be formed, for example, by etching, depositing micrometer scale particles, or photolithography on a suitable substrate.

A lock-in step can prevent further changes in the structure of the porous multilayer. The lock-in can be achieved by, for example, exposure of the multilayer to chemical or thermal polymerization conditions. The polyelectrolytes can become cross-linked and unable to undergo further transitions in porosity. In some cases, chemical crosslinking step can include treatment of a polyelectrolyte multilayer with a carbodiimide reagent. The carbodiimide can promote the formation of crosslinks between carboxylate and amine groups of the polyelectrolytes. A chemical crosslinking step can be preferred when the polyelectrolyte multilayer is formed on a substrate that is unstable at temperatures required for crosslinking (such as, for example, when the substrate is polystyrene). The crosslinking step can be a photocrosslinking step. The photocrosslinking can use a sensitizer (e.g., a light-sensitive group) and exposure to light

(such as UV, visible or IR light) to achieve crosslinking. Masks can be used to form a pattern of crosslinked and non-crosslinked regions on a surface. Other methods for crosslinking polymer chains of the polyelectrolyte multilayer are known.

Nanoparticles can be applied to the multilayer, to provide a nanometer-scale texture or roughness to the surface. The nanoparticles can be nanospheres such as, for example, silica nanospheres, titania nanospheres, polymer nanospheres (such as polystyrene nanospheres), or metallic nanospheres. The nanoparticles can be metallic nanoparticles, such as gold or silver nanoparticles. The nanoparticles can have diameters of, for example, between 1 and 1000 nanometers, between 10 and 500 nanometers, between 20 and 100 nanometers, or between 1 and 100 nanometers. The intrinsically high wettability of silica nanoparticles and the rough and porous nature of the multilayer surface establish favorable conditions for extreme wetting behavior.

A surface can be coated with a hydrophobic material. In general, any hydrophobic material that can be applied over the surface can be used. A material that reacts chemically or physically with a polyelectrolyte multilayer can be used. The hydrophobic material can be chemically bonded to the multilayer, to the nanoparticles, or to both. The hydrophobic material can be a polymeric material, such as a poly(tetrafluoroethylene) or a hydrophobic polysiloxane. The hydrophobic material can be a fluoropolymer, or a fluorosilane. The hydrophobic material can be applied to the surface by a vapor deposition process, e.g., chemical vapor deposition (CVD) or hot filament chemical vapor deposition (HFCVD). See, for example, Lau, K.K.S. *et al., Nano Lett.* **2003**, *3*, 1701, which is incorporated by reference in its entirety.

Superhydrophilic coatings can be created from multilayers without the need for treating the multilayer to induce a porosity transition. For example, the multilayer can include a polyelectrolyte and a plurality of hydrophilic nanoparticles. By choosing appropriate assembly conditions, a 3D nanoporous network of controllable thickness can be created with the nanoparticles. The network can be interconnected - in other words, the nanopores can form a plurality of connected voids. Rapid infiltration (nano-wicking) of water into this network can drive the superhydrophilic behavior.

Examples

Multilayers assembled from poly(allylamine hydrochloride) (PAH) and poly(acrylic acid) (PAA) with the PAH dipping solution at a pH of 7.5 or 8.5 and the

PAA dipping solution at a pH of 3.5 (designated PAH/PAA 7.5/3.5 or 8.5/3.5) formed microporous structures when treated at pH 2.4 followed by a deionized water rinse. See, for example, Mendelsohn, J. D. et al. *Langmuir* **2000**, *16*, 5017; and Hiller, J. *et al.* *Nature Materials* **2002**, *11*, 59, each of which is incorporated by reference in its entirety. The rms surface roughness of these films after treatment was below 100 nm, too low to promote stable superhydrophobic behavior. By using an appropriate combination of acidic treatments, PAH/PAA 8.5/3.5 films were induced to form pores of a size on the order of 10 micrometers and a honeycomb-like structure on the surface. The rms surface roughness of such films can be more than 400 nm, making them ideally suited for use as the high roughness template of a superhydrophobic surface. It can be preferable not to rinse the film with water after low pH treatment. A staged low pH treatment can be preferable to a single low pH treatment.

PAH (M_w = 70,000) was obtained from Sigma-Aldrich (St. Louis, MO). PAA (M_w = 90,000) and silica nanoparticles were obtained from Polysciences (Warrington, PA). (Tridecafluoro-1, 1, 2, 2-tetrahydrooctyl)-1-trichlorosilane was obtained from United Chemical Technology, Inc. Deionized water (>18 MΩ cm, Millipore Milli-Q), with an unadjusted pH of approximately 5.5, was exclusively used in all aqueous solutions and rinsing procedures.

Polyelectrolyte multilayers were assembled on glass microscope slides or 3-aminopropyltriethoxysilane coated microscope slides (LabScientific, Inc.) using an automated Zeiss HMS slide stainer as previously described. (See, for example, Shiratori, S. S.; Rubner, M. F. *Macromolecules* **2000**, *33*, 4213.) Glass substrates were degreased in a detergent solution followed by deionized water rinses prior to multilayer assembly. Silane coated microscope slides were used as received.

PAH/PAA multilayer films were built using pH 8.5 PAH (10^{-2} M by repeat unit) and pH 3.5 PAA (10^{-2} M) aqueous solutions which were pH adjusted by using either 1 M NaOH or 1 M HCl. The first four PAH/PAA bilayers on glass slides were formed by first immersing substrates into the PAH solution for 15 minutes followed by one 2 minute and two 1 minute immersions into water as rinsing steps. Then, the substrates were immersed into the PAA solution for 15 min followed by identical rinsing steps. The remaining layers were assembled by immersion into the polyelectrolyte solutions for 30 seconds followed by one 1 minute and two 30 second immersions into water as rinsing steps. The adsorption and rinsing steps were repeated until the desired numbers of bilayers were

obtained. One bilayer is defined as a single adsorption of a polycation followed by an adsorption of a polyanion; thus a half-integer number of bilayers of PAH/PAA ends with PAH as the outermost layer. A low pH treatment (for example, at a pH of less than pH 5, less than pH 4, between pH 0 and pH 4, or between pH 2 and pH 3)of the polyelectrolyte multilayer introduced pores in the multilayer. The low pH treatment can be a one step treatment or a multistep treatment. For example, a two step treatment can include treatment of the multilayer a pH 2.7 solution and a pH 2.3 solution. The polyelectrolyte multilayers were crosslinked by a 2 hour heat treatment at 180 °C.

1.5 bilayers of silica nanoparticles/PAH were deposited on the crosslinked porous multilayer films using a 0.06 % aqueous colloidal dispersion of silica nanoparticles and pH 8.5 PAH (10^{-2} M by repeat unit) by first immersing the film into the silica nanoparticle suspension for 5 minutes followed by one 1 minute and two 30 second immersions into water as rinsing steps. Then, the film was immersed into the PAH solution for 5 minutes followed by identical rinsing steps. The film was immersed in the silica nanoparticle solution again for 5 minutes followed by one 1 minute and two 30 second immersions into water as rinsing steps.

The silane treatment was carried out by a chemical vapor deposition of (tridecafluoro-1,1,2,2-tetrahydrooctyl)-1-trichlorosilane. Samples were placed in a vacuum chamber together with (tridecafluoro-1,1,2,2-tetrahydrooctyl)-1-trichlorosilane. CVD was performed by applying a 1 Torr vacuum to the chamber at room temperature for 2 hours. Then, the samples were placed in an oven and heated at 180 °C for 2 hours.

Figure 1A shows a scanning electron microscope (SEM) image of a porous PAH/PAA 8.5/3.5 film containing 100.5 assembled bilayers that was created by a single low pH treatment (6 hour immersion in a pH 2.3 solution, with no water rinse). The resultant film exhibits surface pores on the order of 0.5-2 microns and an RMS surface roughness of about 100 nm. In contrast, a 100.5 bilayer PAH/PAA 8.5/3.5 porous film created by a combination of two low pH treatments (i.e., a 2 hour immersion in a pH 2.7 solution followed by a 4 hour immersion in a pH 2.3 solution, with no water rinse) had a surface roughness of about 440 nm (Figure 1B). This film exhibits a honeycomb-like texture with sharp ridges and surface pores as large as 10 micrometers. The surface roughness decreased dramatically when a water rinse (pH about 5.5) followed these low pH treatments.

The two porous PAH/PAA 8.5/3.5 films with micrometer-scale surface roughness were used as templates for nanoparticle deposition. Both structures were first thermally crosslinked at 180 °C for two hours to preserve desirable surface morphological features throughout the subsequent processing steps (see Dai, J. *et al. Langmuir* **2001**, *17*, 931, which is incorporated by reference in its entirety). Nanoscale texture was introduced by depositing 50 nm SiO_2 nanoparticles onto the surfaces via alternating dipping of the substrates into an aqueous suspension of the negatively charged nanoparticles and an aqueous PAH solution followed by a final dipping of the substrates into the nanoparticle suspension. The surfaces were then modified by a chemical vapor deposition (CVD) of (tridecafluoro-1,1,2,2-tetrahydrooctyl)-1-trichlorosilane (semifluorinated silane) followed by a 2 hour heating at 180 °C to remove unreacted semifluorinated silane. These final steps rendered the entire surface hydrophobic.

Dynamic contact angle measurements were carried out on the two types of structures depicted in FIG. 1 after each treatment step to reveal the relationship between contact angle and surface morphology and chemistry. Figure 2 shows the dynamic contact angles measured from structure A (i.e., the structure depicted in Figure 1A) and structure B (i.e., the structure depicted in Figure 1B) at various stages of the process. Both advancing (black bars) and receding (grey bars) contact angles were measured from as-assembled dense films, crosslinked microporous films, and fully treated microporous films, each with and without the surface bound SiO_2 nanoparticles (structures with SiO_2 nanoparticles are indicated by *). At each treatment step, the advancing contact angle measured from structure B was larger than that measured from structure A, consistent with the predictions of both the Wenzel and Cassie models (for a given chemical composition, rougher surfaces exhibit larger advancing contact angles). The deposition of hydrophilic silica nanoparticles onto the surfaces of both crosslinked structures caused the advancing contact angle to decrease, since the surfaces were covered with more wettable hydrophilic groups. After the deposition of the semifluorinated silane and heating, all surfaces changed from hydrophilic to hydrophobic with large advancing contact angles (>120°).

Among the surfaces coated with semifluorinated silane, superhydrophobic character (advancing contact angle > 150°) was observed from all surfaces except structure A without nanoparticles. A low contact angle hysteresis was exhibited by structure B coated with nanoparticles. In this case, water droplets freely rolled off the

surface without becoming pinned even after sitting on the surface for long times. In contrast, water droplets on the surfaces of structure A coated with nanoparticles and on the surface of structure B without nanoparticles started to become pinned after sitting on the surface for a couple of minutes, suggesting a transition from the Cassie state to the Wenzel state. Both the microstructure created by the combined acid treatments and the nanostructure induced by the deposition of nanoparticles can be important for the formation of stable superhydrophobic surfaces.

FIG. 3A shows a high resolution SEM image of the final superhydrophobic surface fabricated from structure B. The nanoparticles decorated the surface of the micropores, forming a two-level structure that conceptually mimics the lotus leaf surface. FIG. 3B shows a water droplet on this surface, having an advancing contact angle of 172°. The lowest angle needed to induce sliding of a 4 mg water droplet on this surface was less than 2°, which suggests a very small contact angle hysteresis with essentially no pinning of the water droplet. This surface remained superhydrophobic after being immersed in water for at least a week, or after being stored in a high humidity environment for at least a month. This stands in contrast to the superhydrophobic surface created from structure A (A3* in Figure 2), which lost its superhydrophobic character after a brief immersion in water.

X-ray photoelectron spectroscopy (XPS) confirmed that the superhydrophobic surface of structure B was modified with the semifluorinated silane (FIG. 4). The XPS spectrum of the crosslinked porous multilayer film with silica nanoparticles showed no detectable fluorine peaks (FIG. 4A), whereas the spectrum of the semifluorinated silane coated film displayed a strong fluorine peak at 688 eV (FIG. 4B). This strong fluorine peak suggests the formation of a polymerized silane film on the surface that is thicker than a single monolayer. The silicon peaks located at 156 eV and 103 eV in FIG. 4A are attributed to the silica nanoparticles deposited on the surface of the crosslinked multilayer film. After the CVD of (tridecafluoro-1, 1, 2, 2-tetrahydrooctyl)-1-trichlorosilane and the subsequent thermal treatment, the intensity of these peaks increased due to the formation of the polymerized silane film (FIG. 4B). In addition to reacting with the silica nanoparticles, the semifluorinated silane can also react with free amine groups on the surface of the crosslinked multilayer film. This was confirmed by examining the XPS spectrum of a porous crosslinked film without nanoparticles after CVD and thermal treatment: a strong fluorine peak located at 688 eV was also observed in this case.

A straight-forward procedure can create stable superhydrophobic coatings from polyelectrolyte multilayers. It is possible to coat any substrate or object amenable to the layer-by-layer deposition process, which is essentially all surfaces. Superhydrophobic coatings can be prepared from PAH/PAA multilayers with as few as 20 bilayers and with shorter treatment and crosslinking times.

A 20.5 bilayer PAH/PAA (7.5/3.5) film was immersed in a pH 2.7 solution for 20 minutes and a pH 2.3 solution for 40 minutes. The film was then dried with air and crosslinked at 180 °C for 2 hours. An additional 3.5 bilayers of PAH/silica nanoparticles were deposited on the surface, followed by CVD of semifluorinated silane. After a 2 hour heat treatment at 180 °C, the surface was superhydrophobic.

Superhydrophobic coatings were successfully made on fibers.

Semifluorinated silane was deposited on acid treated films bearing silica nanoparticles by immersing the samples into 0.4 % (v/v) isopropanol solution of (tridecafluoro-1,1,2,2-tetrahydrooctyl)-1-trichlorosilane for 5 seconds, or by spin coating a 2 % (v/v) isopropanol solution of (tridecafluoro-1,1,2,2-tetrahydrooctyl)-1-trichlorosilane. Superhydrophobic surfaces were obtained after heating the films at 130 °C for 10 minutes.

A superhydrophobic surface was patterned with hydrophilic regions by printing 0.25% (w/v) isopropanol solutions of poly(acrylic acid) on the superhydrophobic surfaces using an Epson inkjet print or a cotton swab. This can also be achieved by using a 2 % (w/w) isopropanol solution of titanium (IV) isopropoxide.

The multilayers can be superhydrophilic prior to coating with a hydrophobic material. The superhydrophilic behavior is characterized by nearly instantaneous wetting by water, and advancing and receding contact angles differ by less than 5°. Thus, this approach can create both superhydrophobic and superhydrophilic coatings with identical surface morphologies but with dramatically different wetting characteristics. A surface can include both superhydrophobic and superhydrophilic regions. The superhydrophobic and superhydrophilic regions can form a pattern on the surface. Such a patterned surface could be useful, for example, in a microfluidic device.

The superhydrophobic surface can trap a layer of air at the superhydrophobic surface when submerged under water. Because of the difference in refractive indices between water and air, this air layer can act as a mirror.

To prepare a superhydrophilic surface, four bilayers of alternating PAH and SPS were assembled at pH 4.0 onto a glass surface. The four bilayers promoted adhesion of subsequently added layers to the surface, but did not influence the superhydrophilic behavior of the final surface. Colloidal silica nanoparticles where then alternately assembled with PAH to complete the coating. The assembly process was driven by electrostatic interactions between the PAH polycation and the negatively charged SiO_2 nanoparticles.

Coatings were prepared with three different sizes of colloidal silica nanoparticles to investigate the effect of particle size on coating properties. Specifically, nanoparticles with diameters of 7 nm (Ludox SM 30), 12 nm (Ludox HS 40), and 22 nm (Ludox TM 40) were used. The pH of the PAH and silica nanoparticles solutions was varied from 3.0 to about 10 to determine processing conditions that promote formation of stable superhydrophilic coatings. For 12 nm and 22 nm nanoparticles, multilayer films having more than 8 bilayers of PAH/SiO_2 became cloudy at a pH of less than 9, due to aggregation of the nanoparticles. Multilayer films assembled with 7 nm nanoparticles, on the other hand, remained highly transparent even after the deposition of 16 PAH/SiO_2 bilayers. Clouding of these films only began to appear when 24 or more bilayers had been deposited. Preferred conditions for superhydrophilic multilayers were 7 nm SiO_2 nanoparticles, pH 4 or pH 8-9, and at least 8 bilayers. The source of silica nanoparticles can be important for obtaining superhydrophilic behavior. Films prepared with nanoparticles obtained from other sources were of lower quality.

The concentration of the SiO_2 nanoparticle solution used in forming the layers influenced final film properties. Concentrations in the range of 0.005% to 0.1% by weight were tested. At the extremes of the range, the resulting films were not superhydrophilic. Desirable film properties were obtained with a nanoparticle concentration in the range of 0.01% to 0.03% by weight. In this range, the thickness of the resulting film increased approximately linearly with number of bilayers deposited (see FIG. 5A). FIG. 5A displays thickness data for $(PAH4.0/SiO_24.0)_x$ multilayer films. The average bilayer growth increment (average thickness deposited per bilayer) for multilayers assembled at this pH from the 0.03% nanoparticle concentration solution was 18 nm/ bilayer. The bilayer growth increment for multilayer films assembled with SiO_2 nanoparticles can be influenced by a complex interplay of parameters such as particle charge, concentration and aggregation and the charge density of the polycation. Such

parameters have been explored in detail in the literature. See, for example, Lvov, Y.; et al. *Langmuir* 1997, 13, (23), 6195-6203; and Lvov, Y. M.; et al. *Chemical Communications* 1998, (11), 1229-1230, each of which is incorporated by reference in its entirety. The refractive index of the film decreased with number of bilayers deposited (see FIG. 5B). All the films described in FIG. 5B exhibited a low refractive index in the range of 1.246 to 1.270. The lowest refractive index was obtained with a film having 14 bilayers fabricated with a 0.03% by weight solution of silica nanoparticles. Low refractive index is important for effective antireflective behavior, and can be a result of porosity in the film introduced by the packing arrangement of the nanoparticles.

FIG. 5C shows how the thickness and refractive index vary as a function of the number of deposited bilayers for films assembled at a higher pH (PAH 7.5/ SiO_2 9.0)$_x$. Also included in this figure are data for calcinated films (see below). Using the optimum particle concentration (0.03%), the average bilayer thickness increment was about 7.7 nm/bilayer and refractive index values fell in the range of 1.23-1.26 for films with 14-20 bilayers. Compared to multilayer films assembled at lower pH (pH 4.0), the higher pH assembled nanoparticle multilayers exhibited a smaller bilayer thickness increment, but, at a given film thickness, somewhat lower refractive index values. The effective optical thickness of a multilayer (i.e., product of thickness and refractive index) determined the number of bilayers needed to achieve the suppression of surface reflections at a desired wavelength.

FIG. 6 shows an AFM image of 12 PAH/SiO_2 bilayer film (PAH 7.5/SiO_2 8.0)$_{12}$ assembled from a 0.03% by weight nanoparticle solution. In the image, clearly aggregated nanoparticles can be see, that create hill-to-valley surface cavities that typically extend at least about 40-60 nm into the film as revealed by a cross-section thickness trace. The rms surface roughness was in the range of 12-16 nm.

The low refractive index resulting from the porous nature of the PAH/SiO_2 multilayer films gave rise to anti-reflection properties. For a glass substrate with a refractive index of about 1.5, the maximum suppression of reflective losses occurs when an anti-reflection coating has a refractive index of 1.22. The wavelength of maximum suppression is determined by the quarter-wave thickness of the coating. The quarter-wave thickness of a multilayer coating, in turn, can be tuned throughout the entire visible range and beyond by simply controlling the number of deposited bilayers. Measurements reveal (FIG. 7) that transmission levels in excess of 99% were achieved in the visible

region (400 to 700 nm). For example, an 8 bilayer PAH 4.0/SiO_2 4.0 multilayer film (thickness 97 nm) transmitted 99.6% of incident light at a wavelength of 490 nm. Without the anti-reflection coating, this glass transmitted about 92% of incident light. The ability of thin film coatings based on PAH/SiO_2 multilayers to effectively suppress reflective losses was further illustrated by multilayers assembled at PAH 7.5/SiO_2 9.0 (FIG. 8). At the optimum wavelength determined by the quarter-wave film thickness, reflective losses as low as about 0.1% and transmission levels of 99.7% were readily achieved. The wavelength range of maximum suppression for all of these films was much broader than what would be expected from a single index quarter-wave anti-reflection coating (determined by comparisons with optical simulations). This indicates that a gradient refractive index profile was established in the film as a result of the nano-corrugated surface topography. See, e.g, Hiller, J.; Mendelsohn, J.; Rubner, M. F. *Nature Mater.*, **2002**, 1, 59, which is incorporated by reference in its entirety.

As indicated in FIGS. 7 and 8, the thickness per deposited bilayer in the case of PAH/SiO_2 multilayer films fabricated from 7 nm diameter SiO_2 nanoparticles was small enough to allow the fabrication of a family of films with quarter-wave thicknesses that span the entire visible range. This level of fine-tuning is more difficult to achieve with anti-reflection coatings based on a single layer of adsorbed silica nanoparticles. See, for example, Zhang, X-T.; et al. *Chem. Mater.* **2005**, 17, 696; Hattori, H. *Adv. Mater.* **2001**, *13*, 51; Koo, H. Y.; et al. *Adv. Mater.* **2004**, *16*, 274; and Ahn, J. S.; et al. *Colloids and Surfaces A: Physicochem. Eng. Aspects* **2005**, *259*, 45, each of which is incorporated by reference in its entirety. In addition, these results showed that coatings containing many layers of very small nanoparticles were more effective at suppressing reflections than single layer coatings fabricated from larger nanoparticles (99.7 % versus 98.8 % transmission).

A key attribute of any practical anti-fogging/anti-reflection coating is excellent mechanical durability and adhesion. The PAH/SiO_2 multilayer films as-prepared exhibit adhered well and exhibited mechanical integrity, but could be rubbed off with aggressive mechanical action. The mechanical stability of these films, however, was increased tremendously by heating the film to about 500 °C for four hours. This calcination process burns out the polymer component of the film and fuses the silica nanoparticles together via the formation of stable siloxane bridges. See, for example, Unger, K. K., *Porous silica: its properties and use as support in column liquid chromatography*. Elsevier

Scientific Pub. Co.: Amsterdam; New York, 1979; p xi, 336, which is incorporated by reference in its entirety. After this process, the resultant thin film coating was able to withstand aggressive rubbing treatments and easily passed a standard scotch tape peel test (some glue residue remained on the surface, but could be removed with solvents or plasma treatment). In addition, a negligible amount of the film was removed by scratching the surface with a razor blade. This process, of course, was only possible when the multilayer films are assembled on a substrate that can withstand this high treatment temperature.

FIG. 5C shows that the thickness of an as-assembled PAH/SiO_2 multilayer film decreased by only a small amount after calcination. The refractive index also decreased, because the high refractive index polymer (ca. 1.5) was removed, thereby increasing the level of void volume in the film. The net result was that the optical properties of the film undergo only small changes after calcination. A comparison of FIGS. 8A and 8B reveals that the wavelength of maximum transmission/minimum reflection shifted slightly to the blue as a result of the decrease in film thickness, and the level of transmission increased due to the lower refractive index. For example, for a 14 bilayer (PAH 7.5/SiO_2 9.0) film, the wavelength of maximum transmission shifted from 550 nm to 540 nm and the level of transmission increased from 99.7 to 99.8 % after calcination.

Wetting behavior of the films was examined by using a video contact angle instrument operating at 60 frames per second (16.6 ms time interval between frames). For multilayers assembled from a 0.03% by weight nanoparticle solution, at least 14 bilayers were required to create a film that was completely wetted (i.e., contact angle less than 5°) with water in 0.5 seconds or less. See FIG. 9. Surfaces with fewer bilayers are highly wettable but not superhydrophilic. As shown in FIGS. 9B-9C, the wetting time for a second drop added to a surface was remarkably fast. Still images obtained from video data indicated that a first drop of water can wet the surface in 0.16 seconds, and a second drop in the same location spreads completely in 0.03 seconds.

In contrast to superhydrophilic surfaces based on TiO_2, the superhydrophilic behavior of PAH/SiO_2 multilayer films is stable for extended periods of time, in light or dark conditions, even at elevated temperatures. See FIG. 10. A sixteen bilayer (PAH 7.5 / SiO_2 8.0) film stored at room temperature in the dark displayed no significant change in wetting behavior over a period of at least one year. The films appeared to be stable indefinitely under these conditions. At elevated temperatures, some films (12 bilayers of

PAH7.5/$SiO_2$8.0 with 10 bilayers of PAH/PAA as adhesion layers (0.03% by wt silica solution) retained their superhydrophilic behavior for at least 168 hours at 50 °C and about 144 hours at 80 °C. Anti-fogging behavior (see below) was retained by all films heated at 50°C for 168 hours. At the highest temperature examined, the more dramatic loss in superhydrophilicity observed with certain films at long times (> 144 hours) may reflect the formation of siloxane bridges formed by the condensation of surface silanol groups by thermal dehydroxylation. See, for example, Unger, K. K., *Porous silica: its properties and use as support in column liquid chromatography*. Elsevier Scientific Pub. Co.: Amsterdam; New York, 1979; p xi, 336 p, which is incorporated by reference in its entirety. Dehydroxylation would render the SiO_2 nanoparticles more hydrophobic. The superhydrophilic behavior of films treated for long times at elevated temperatures could be completely recovered by treatment for 30 seconds in an oxygen plasma. This observation is consistent with the notion that the surface chemistry of the particles was altered at elevated temperature. From these tests, however, the possibility that the coatings became contaminated in the oven cannot be ruled out. It should be noted that the anti-reflection properties of these films did not change as a result of heat treatments. In addition, no significant differences in wetting behavior were observed between as-prepared and calcinated samples..

As expected, a surface with a water droplet contact angle of essentially zero exhibited anti-fogging characteristics due to the fact that the nearly instantaneous, sheet-like wetting by water prevented light-scattering water droplets from forming on the surface. FIG. 10 indicates that anti-fogging behavior persisted as long as the water droplet contact angle was below about 7°. The images in FIG. 11 illustrate this effect. FIG. 11A shows two glass sides resting atop a photograph of a lotus flower. The slide to the left had a superhydrophilic coating; the slide on the right was without such a coating. Both slides were cooled in a refrigerator at about -18 °C and then moved into humid laboratory air. The uncoated slide fogged immediately whereas the coated slide remained clear. Another interesting characteristic of a superhydrophilic coating is its ability to prevent dewetting by water. As soon as a typical glass slide is withdrawn from water, the well-known dewetting phenomenon takes place (see Figure 11B). In sharp contrast, a glass slide coated with a superhydrophilic multilayer remains fully wet after immersion in water and stays in this state until the water evaporates.

Other embodiments are within the scope of the following claims.

WHAT IS CLAIMED IS:

1. A superhydrophilic surface comprising a nanotextured coating including a hydrophilic material arranged on a substrate.

2. The surface of claim 1, wherein the substrate is substantially transparent.

3. The surface of claim 2, wherein the surface is substantially transparent.

4. The surface of claim 3, wherein the surface has a refractive index of less than 1.4.

5. The surface of claim 4, wherein the surface has a refractive index of less than 1.3.

6. The surface of claim 3, wherein the coating has a thickness of less than 500 nm.

7. The surface of claim 3, wherein the coating has a thickness of less than 300 nm.

8. The surface of claim 3, wherein the surface has an rms roughness in the range of 10-20 nm.

9. The surface of claim 3, wherein the surface has an rms roughness in the range of 12-16 nm.

10. The surface of claim 1, wherein the coating includes a plurality of nanoparticles.

11. The surface of claim 10, wherein the plurality of nanoparticles includes a silica nanoparticle.

12. The surface of claim 10, wherein the plurality of nanoparticles includes a nanoparticle having a diameter in the range of 5 nm to 100 nm.

13. The surface of claim 10, wherein the plurality of nanoparticles includes a nanoparticle having a diameter in the range of 5 nm to 25 nm.

14. The surface of claim 10, wherein the coating is substantially free of organic polymer.

15. The surface of claim 10, wherein the coating includes a polyelectrolyte.

16. The surface of claim 15, wherein the polyelectrolyte includes a polycation.

17. The surface of claim 15, wherein the polyelectrolyte includes poly(allylamine hydrochloride).

18. The surface of claim 15, wherein the coating further comprises a bilayer, the bilayer including a polyelectrolyte having a charge and a material having an opposite charge.

19. The surface of claim 18, wherein the material having the opposite charge is a polyelectrolyte.

20. The surface of claim 18, wherein the material having the opposite charge is a plurality of nanoparticles.

21. A method of treating a surface comprising:

forming a coating on a surface of a substrate, wherein the coating includes a bilayer including a polyelectrolyte having a charge and a second material having an opposite charge.

22. The method of claim 21, wherein the second material is hydrophilic.

23. The method of claim 21, wherein the second material includes a polyelectrolyte.

24. The method of claim 21, wherein the second material includes a nonpolymeric material.

25. The method of claim 21, wherein the second material includes a plurality of nanoparticles.

26. The method of claim 21, further comprising sequentially forming a plurality of bilayers, wherein each bilayer includes a polyelectrolyte having a charge and a second material having an opposite charge.

27. The method of claim 26, wherein at least one bilayer includes a polyelectrolyte.

28. The method of claim 26, wherein at least one bilayer includes a nonpolymeric material.

29. The method of claim 26, wherein at least one bilayer includes a plurality of nanoparticles.

30. The method of claim 21, wherein forming the bilayer includes contacting the surface of the substrate with an aqueous solution of the polyelectrolyte.

31. The method of claim 21, wherein forming the bilayer includes contacting the surface of the substrate with an aqueous solution of the second material.

32. The method of claim 21, further comprising heating the coating.

33. The method of claim 21, further comprising contacting the coating with a plasma.

34. A method of manufacturing an antifogging surface comprising forming a nanotextured layer including a hydrophilic material arranged on a surface of a substrate.

35. An article comprising a surface having an antireflective coating including a nanotextured hydrophilic material.

36. An article comprising a surface having an antifogging coating including a nanotextured hydrophilic material.

37. The article comprising a superhydrophobic surface patterned with hydrophilic regions.

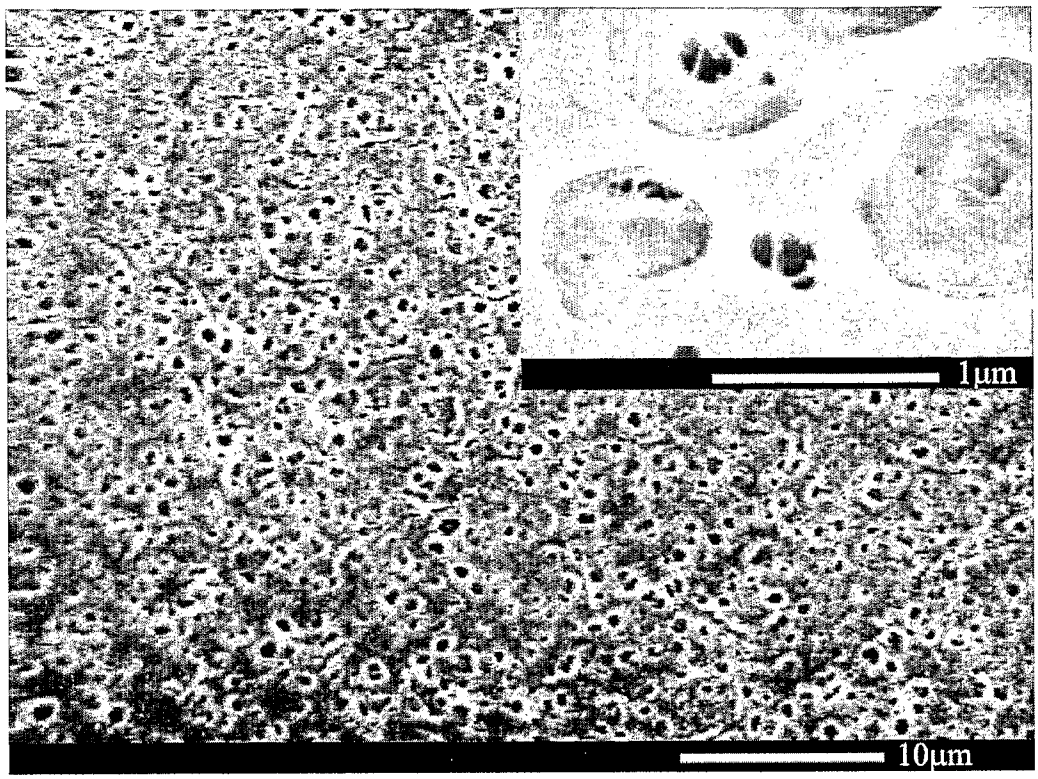

FIG. 1A

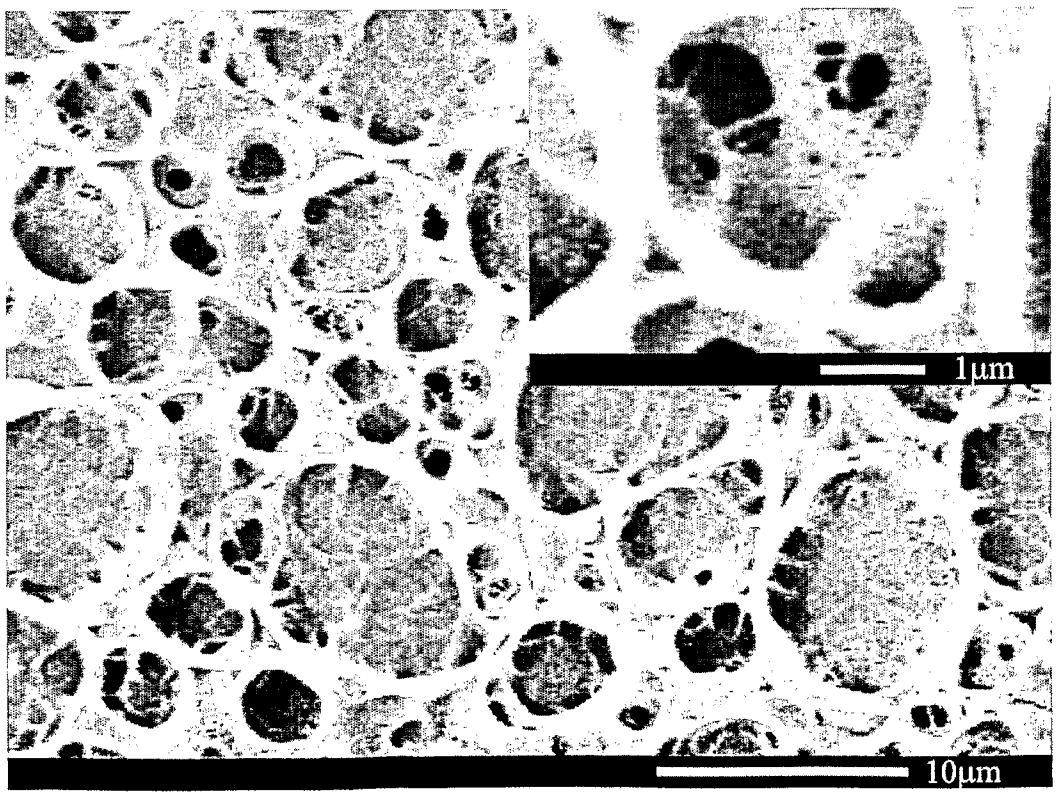

FIG. 1B

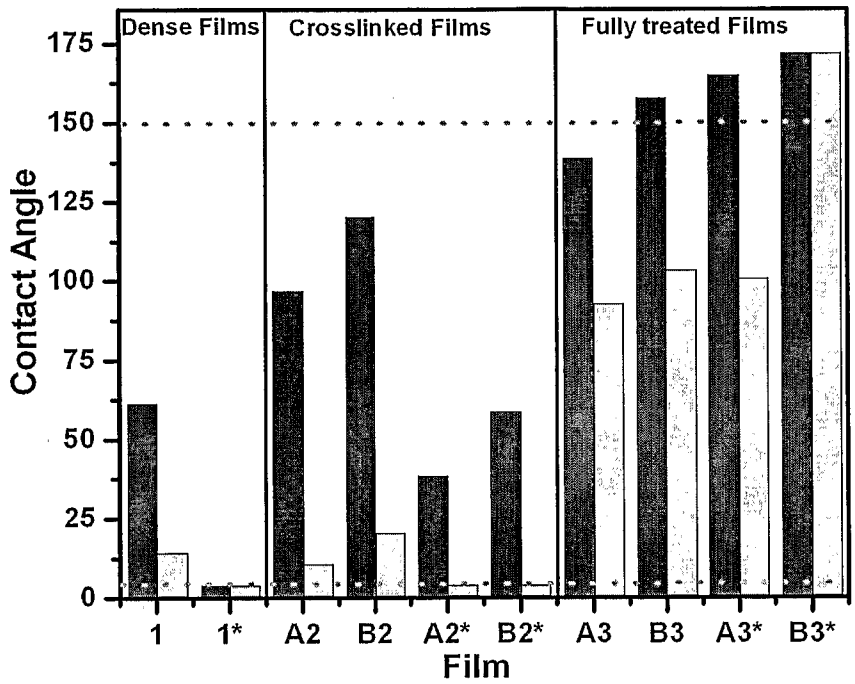
Dense Films
Crosslinked Films
Fully treated Films
Contact Angle
175
150
125
100
75
50
25
0
1
1*
A2
B2
A2*
B2*
A3
B3
A3*
B3*
Film

FIG. 2

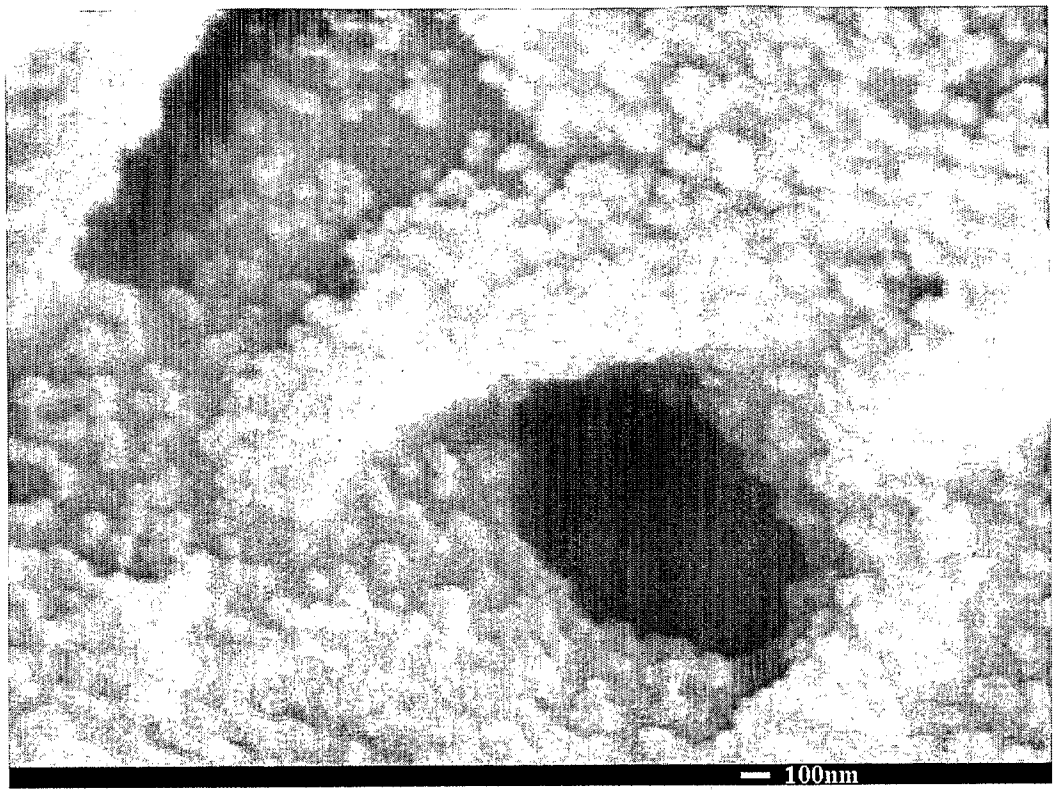

FIG. 3A

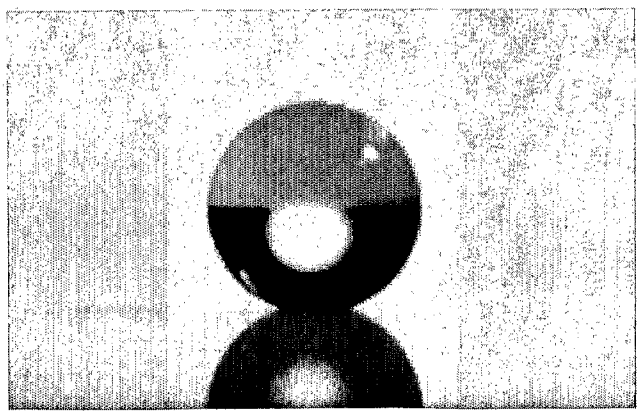

FIG. 3B

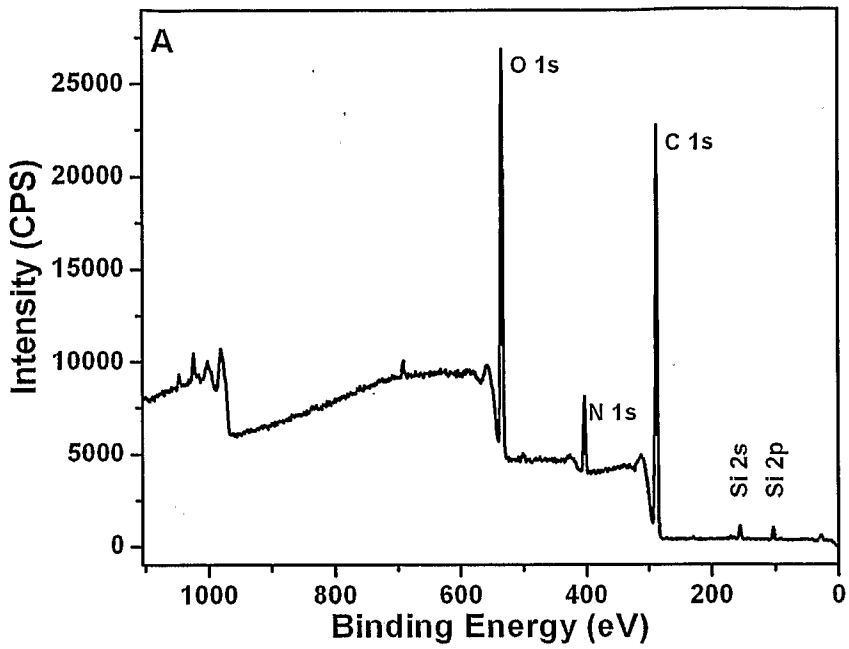
A
O 1s
C 1s
N 1s
Si 2s
Si 2p
Intensity (CPS)
25000
20000
15000
10000
5000
0
1000
800
600
400
200
0
Binding Energy (eV)

FIG. 4A

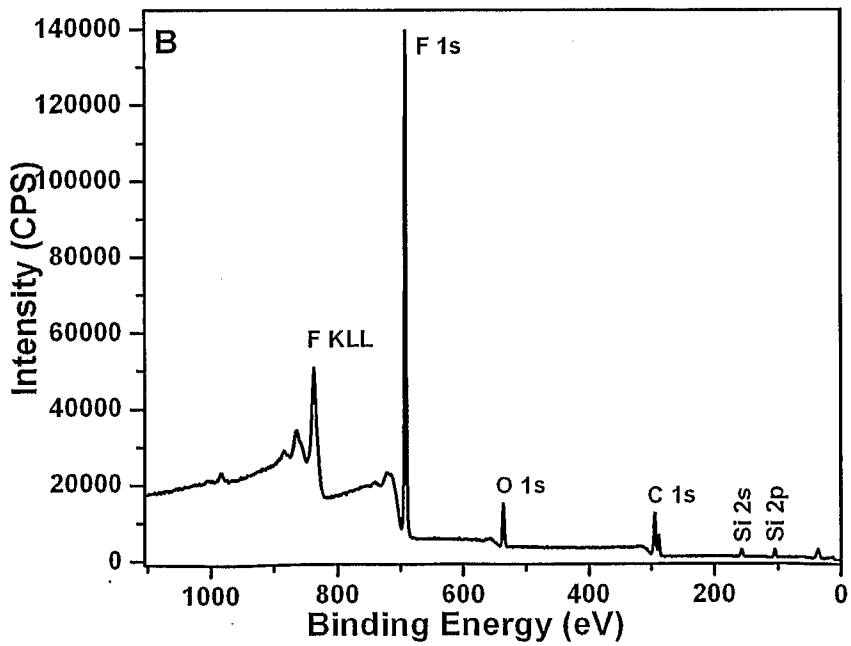
B
F 1s
F KLL
O 1s
C 1s
Si 2s
Si 2p
Intensity (CPS)
140000
120000
100000
80000
60000
40000
20000
0
1000
800
600
400
200
0
Binding Energy (eV)

FIG. 4B

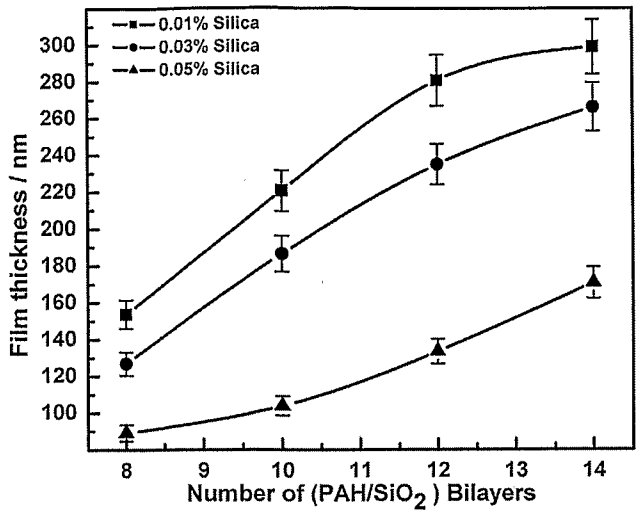
0.01% Silica
0.03% Silica
0.05% Silica
Film thickness / nm
300
280
260
240
220
200
180
160
140
120
100
8
9
10
11
12
13
14
Number of (PAH/SiO2) Bilayers

FIG. 5A

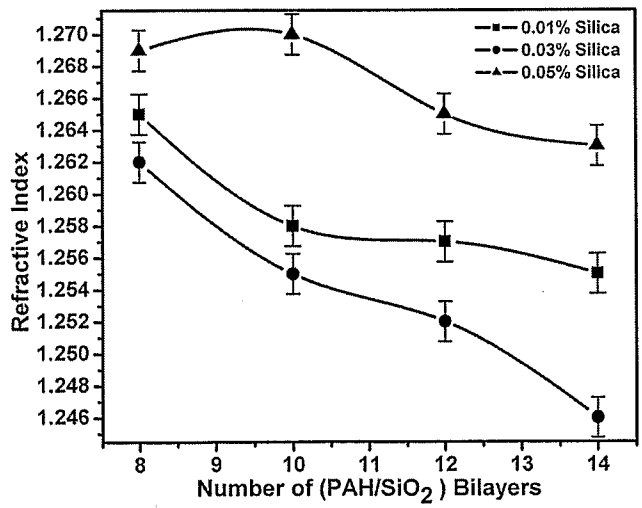
0.01% Silica
0.03% Silica
0.05% Silica
Refractive Index
1.270
1.268
1.266
1.264
1.262
1.260
1.258
1.256
1.254
1.252
1.250
1.248
1.246
8
9
10
11
12
13
14
Number of (PAH/SiO2) Bilayers

FIG. 5B

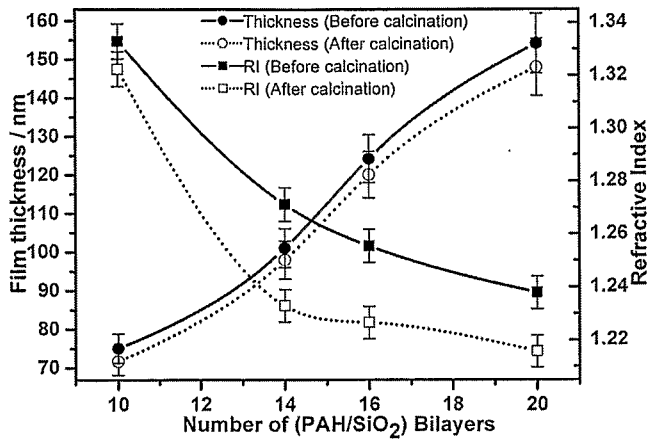
Thickness (Before calcination)
Thickness (After calcination)
RI (Before calcination)
RI (After calcination)
Film thickness / nm
Refractive Index
Number of (PAH/SiO2) Bilayers
160
150
140
130
120
110
100
90
80
70
1.34
1.32
1.30
1.28
1.26
1.24
1.22
10
12
14
16
18
20

FIG. 5C

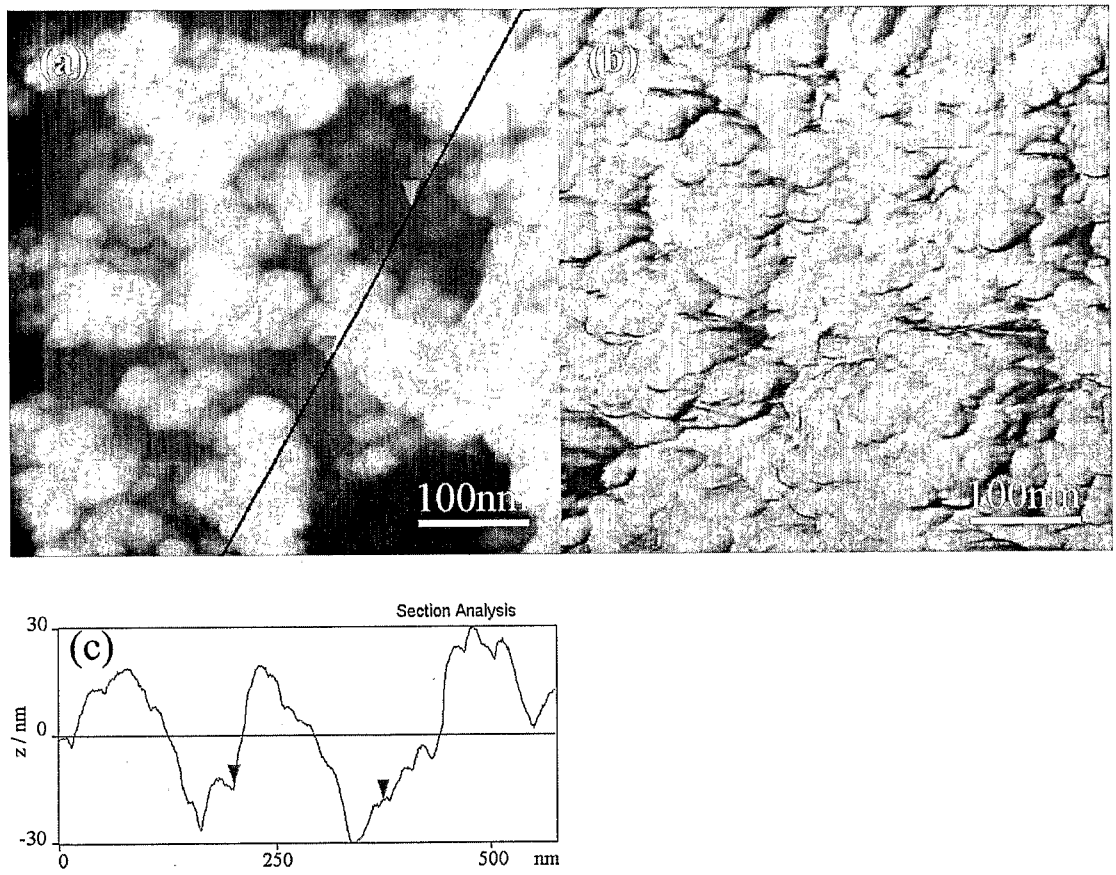

FIG. 6

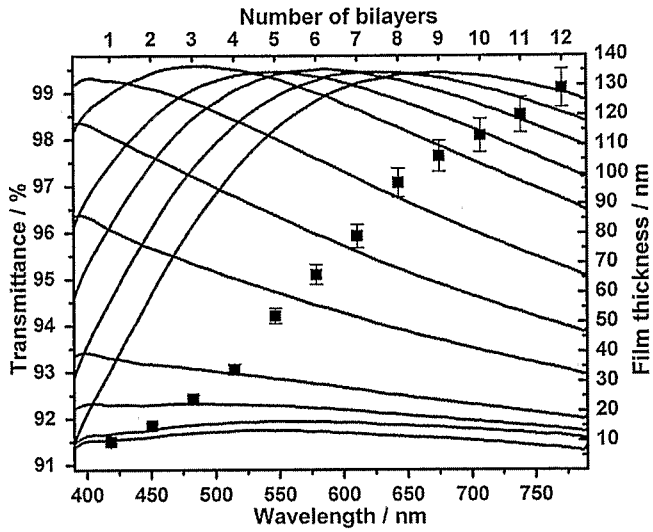
Number of bilayers
1 2 3 4 5 6 7 8 9 10 11 12
Transmittance / %
99 98 97 96 95 94 93 92 91
Film thickness / nm
140 130 120 110 100 90 80 70 60 50 40 30 20 10
400 450 500 550 600 650 700 750
Wavelength / nm

FIG. 7

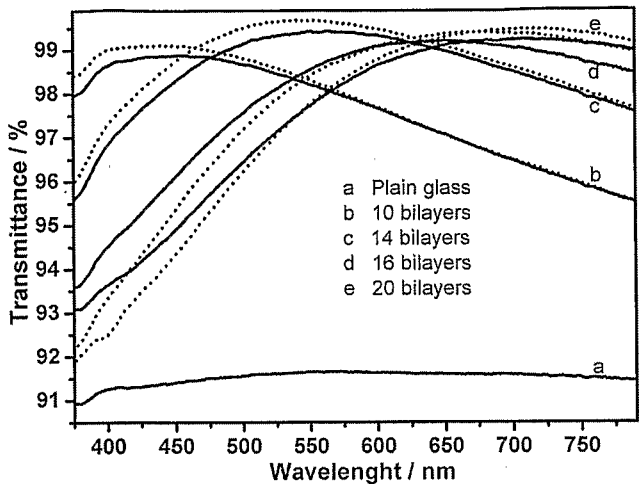
Transmittance / %
Wavelenght / nm
a Plain glass
b 10 bilayers
c 14 bilayers
d 16 bilayers
e 20 bilayers

FIG. 8A

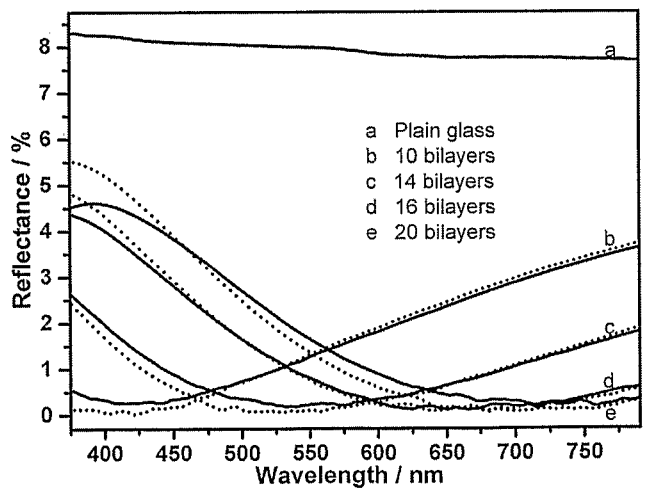
Reflectance / %
Wavelength / nm
a Plain glass
b 10 bilayers
c 14 bilayers
d 16 bilayers
e 20 bilayers

FIG. 8B

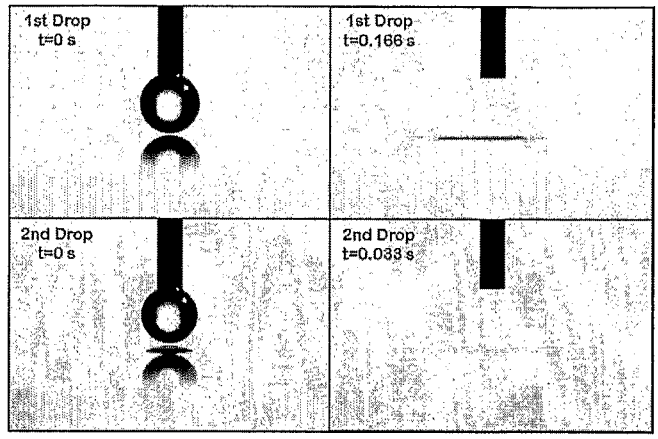
1st Drop
t=0 s
1st Drop
t=0.166 s
2nd Drop
t=0 s
2nd Drop
t=0.033 s

FIG. 9A

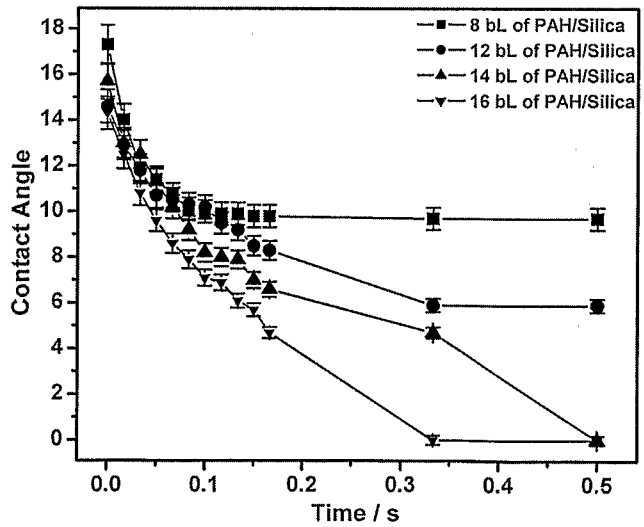
8 bL of PAH/Silica
12 bL of PAH/Silica
14 bL of PAH/Silica
16 bL of PAH/Silica
Contact Angle
Time / s
0
2
4
6
8
10
12
14
16
18
0.0
0.1
0.2
0.3
0.4
0.5

FIG. 9B

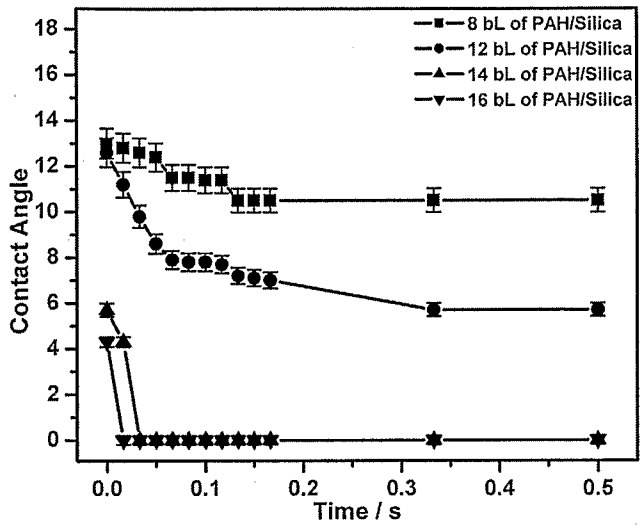
8 bL of PAH/Silica
12 bL of PAH/Silica
14 bL of PAH/Silica
16 bL of PAH/Silica
Contact Angle
Time / s
0
2
4
6
8
10
12
14
16
18
0.0
0.1
0.2
0.3
0.4
0.5

FIG. 9C

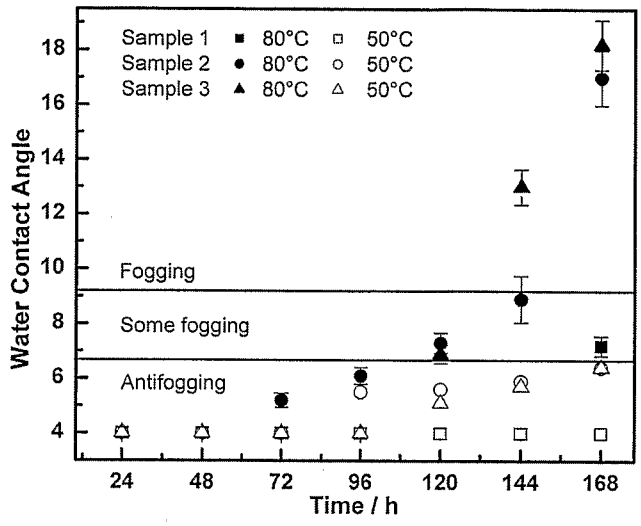
Sample 1 ■ 80°C □ 50°C
Sample 2 ● 80°C ○ 50°C
Sample 3 ▲ 80°C △ 50°C
Fogging
Some fogging
Antifogging
Water Contact Angle
Time / h
4
6
8
10
12
14
16
18
24
48
72
96
120
144
168

FIG. 10

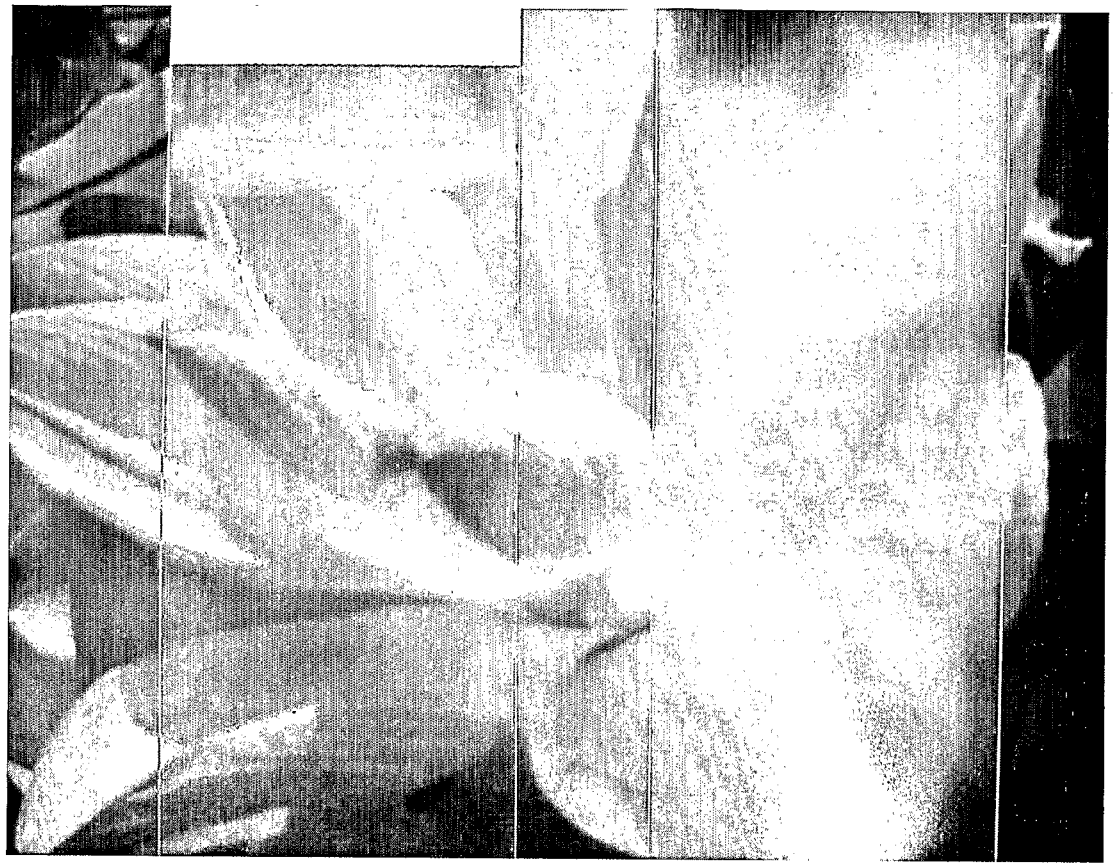

FIG. 11A

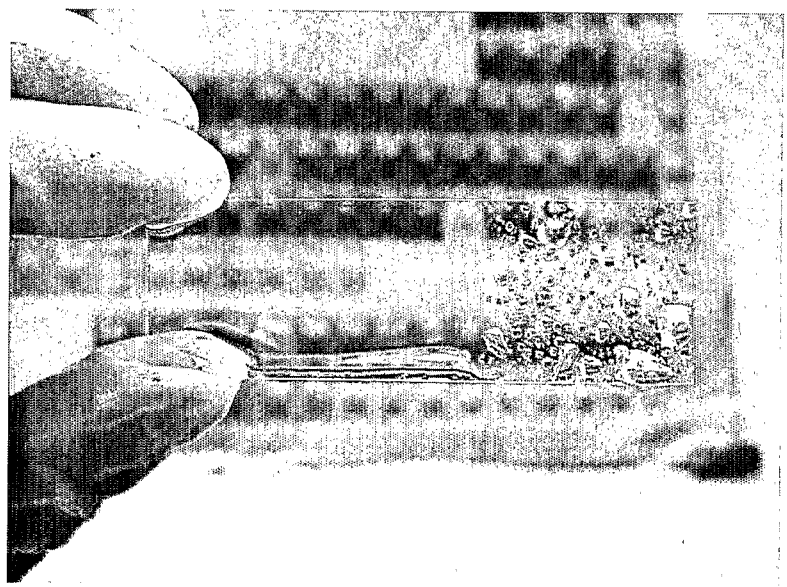

FIG. 11B